

# Rational approximation of the rough Heston solution

Jim Gatheral, Baruch College, CUNY,  
`jim.gatheral@baruch.cuny.edu`

Radoš Radoičić, Baruch College, CUNY,  
`rados.radoicic@baruch.cuny.edu`

January 29, 2019

## Abstract

Pricing in the rough Heston model of [Jaisson & Rosenbaum(2016)] requires the solution of a fractional Riccati differential equation, which is not known in explicit form. Though numerical schemes to approximate this solution do exist, they inevitably require significantly more time to compute than the closed-form solution in the classical Heston model. In this paper, we present a simple rational approximation to the solution of the rough Heston Riccati equation valid in a region of its domain relevant to option valuation. Pricing using this approximation is both fast and very accurate.

## 1 Introduction

Originally obtained in [Jaisson & Rosenbaum(2016)] as the limit of a simple market microstructure model of autocorrelated order flow with a power-law propagator, the rough Heston model may be written as follows.

$$\begin{aligned}\frac{dS_t}{S_t} &= \sqrt{v_t} \{ \rho dW_t + \sqrt{1 - \rho^2} dW_t^\perp \} \\ v_u &= \xi_t(u) + \frac{\nu}{\Gamma(\alpha)} \int_t^u \sqrt{v_s} (u - s)^{\alpha-1} dW_s, \quad u \geq t\end{aligned}\tag{1.1}$$

where  $\xi_t(u) = \mathbb{E}[v_u | \mathcal{F}_t]$ ,  $u > t$  is the forward variance curve and  $\frac{1}{2} < \alpha = H + \frac{1}{2} \leq 1$ . Here,  $H \in (0, 1/2]$  is the Hurst exponent<sup>1</sup>,  $\nu$  is the volatility of volatility, and  $\rho \in [-1, 1]$  is the correlation between spot and volatility moves. The parameter  $H$ , when estimated either from the historical volatility times series or by fitting the model to the implied volatility surface, is found to be small, of the order of 0.1: hence the terminology *rough*.

[El Euch & Rosenbaum(2019)] derived a quasi-closed form expression for the rough Heston characteristic function for the log-stock price analogous to the expression for the classical Heston characteristic function. Specifically [El Euch & Rosenbaum(2019), Abi Jaber *et al.*(2017), Gatheral & Keller-Ressel(2018)], the characteristic function of the terminal log-spot  $X_T$  conditional on the time- $t$  initial state  $(X_t, \xi_t)$  is given by

$$\varphi_t^T(a) = \exp \left\{ i a X_t + \int_t^T D^\alpha h(a, T - u) \xi_t(u) du \right\}, \tag{1.2}$$

---

<sup>1</sup>Paths of the volatility process have Hölder regularity  $H - \epsilon$  for any  $\epsilon > 0$ .

where  $h(a, \cdot)$  is the unique continuous solution of the fractional Riccati equation

$$D^\alpha h(a, t) = -\frac{1}{2} a (a + i) + i \rho \nu a h(a, t) + \frac{1}{2} \nu^2 h^2(a, t); \quad I^{1-\alpha} h(a, 0) = 0. \quad (1.3)$$

Here  $D^\alpha$  and  $I^{1-\alpha}$  represent respectively fractional differential and integral operators (see [A](#) for a very brief introduction to fractional calculus). Equation (1.3) is a rough version of the Riccati equation arising in the classical Heston model (with zero mean reversion); indeed the only difference is that the time derivative is replaced by a fractional derivative. In contrast to the classical Heston case, there is no explicit solution to the Riccati equation (1.3).

Over the last few decades, various techniques have been used to obtain analytical approximations for solutions of fractional differential equations and their integral counterparts, such as Adomian's decomposition method [[Momani & Shawagfeh\(2006\)](#)], the homotopy perturbation method [[Odibat & Momani\(2008\)](#)], the variational iterative method [[Odibat & Momani\(2006\)](#)], the homotopy analysis method [[Cang et al.\(2009\)](#)], and the operational matrix and spectral method based on orthogonal polynomials [[Bhrawy et al.\(2015\)](#)]. Unfortunately, the analytical expressions thus obtained are, without exception, series expansions around zero that approximate the true solution well only for small values of the argument (*i.e.* short times). Whilst the radius of convergence of these short-time expansions is typically unknown, their errors can be seen (numerically) to blow up quickly for large times, making them useless in our context.

The Adams scheme [[Diethelm et al\(2004\)](#)] is the standard numerical method for obtaining solutions of fractional ordinary differential equations for all times. The Adams scheme is essentially an Euler scheme involving a discrete-time convolution induced by the fractional derivative; a large number of steps and significant computation time is required to achieve satisfactory accuracy (see Section 5.1). Such numerical solutions are inevitably much slower to compute than the closed-form classical Heston expression.

In our special case of the rough Heston Riccati equation, [[Callegaro et al.\(2018\)](#)] recently studied the radius of convergence of a specific short-time series expansion and applied Richardson-Romberg extrapolation (outside the convergence domain) to obtain a “promising and encouraging” hybrid numerical scheme for all times.

Finally, in [[Abi Jaber & El Euch\(2018\)](#)], the fractional kernel is approximated by a sequence of exponentially decaying kernels, yielding a sequence of conventional multi-factor stochastic volatility models that is shown to converge to the rough Heston model in a specified region. Numerical experiments show that approximating the rough Heston Riccati equation by an  $n$ -dimensional classical Riccati equation with a large number of factors ( $n = 500$ ) yields good results when compared to the Adams scheme with 200 steps as benchmark.

In this paper, we present accurate global rational approximations to the solution  $h$  of the fractional Riccati equation, valid over a region of the domain of  $h$  of interest, which are at least as fast to compute as the corresponding closed-form classical Heston solution and obviously a huge factor faster and much simpler than any of the alternative approximate solutions mentioned above. Moreover, we show by numerical experiment that our preferred rational approximation is not only much faster but also typically more accurate than the Adams scheme for any reasonable choice of the number of time steps.

Given this approximate solution to the Riccati Equation (1.3), an accurate approximation to the characteristic function (1.2) may be easily computed. European option prices may then be obtained using standard techniques. In particular, in equation (5.6) of [[Gatheral\(2006\)](#)], we have the following representation of the price of a call option in terms of the characteristic

function, originally from [Lewis(2000)]:

$$C(S, K, T) = S - \sqrt{SK} \frac{1}{\pi} \int_0^\infty \frac{du}{u^2 + \frac{1}{4}} \operatorname{Re} \left[ e^{-iuk} \varphi_t^T(u - i/2) \right] \quad (1.4)$$

where  $S$  is the current stock price,  $K$  the strike price and  $T$  expiration. Finally, implied volatilities may be computed by numerical inversion of the Black-Scholes formula. A key observation is that for option pricing with equation (1.4), we need a good approximation to the characteristic function only along the contour  $a = u - i/2$ ,  $u \in \mathbb{R}_{>0}$ . On the other hand, to value the leverage swap, we need to differentiate the characteristic function at  $a = -i$ . Thus we need only find a good approximation to the solution  $h(a, x)$  of the rough Heston Riccati equation for  $a \in \mathcal{A}$  where  $\mathcal{A}$  is a suitable region in the complex plane (see Definition 3.1).

## 1.1 Main results and organization of the paper

Our paper is organized as follows. In Section 2, we derive a short-time expansion of the solution  $h$  of the rough Heston Riccati equation (1.3). Then in Section 3, we derive an asymptotic solution to (1.3) in the long-time limit  $\tau = T - t \rightarrow \infty$ . In Section 4, we show how to construct global rational approximations to  $h$ . Then in Section 5, we present numerical results, highlighting one specific approximate solution that is particularly simple and accurate. Finally, in Section 6, we summarize and conclude. Some technical details are relegated to the appendix.

## 2 Solving the rough Heston Riccati equation for small times

First, we derive a short-time expansion of the solution. From [Alòs et al.(2017)],  $h(a, t)$  can be written as

$$h(a, t) = \sum_{j=0}^{\infty} \frac{\Gamma(1+j\alpha)}{\Gamma(1+(j+1)\alpha)} \beta_j(a) \nu^j t^{(j+1)\alpha} \quad (2.1)$$

with

$$\begin{aligned} \beta_0(a) &= -\frac{1}{2} a(a+i) \\ \beta_k(a) &= \frac{1}{2} \sum_{i,j=0}^{k-2} \mathbb{1}_{i+j=k-2} \beta_i(a) \beta_j(a) \frac{\Gamma(1+i\alpha)}{\Gamma(1+(i+1)\alpha)} \frac{\Gamma(1+j\alpha)}{\Gamma(1+(j+1)\alpha)} \\ &\quad + i\rho a \frac{\Gamma(1+(k-1)\alpha)}{\Gamma(1+k\alpha)} \beta_{k-1}(a). \end{aligned} \quad (2.2)$$

We note that  $\nu h(a, t)$  is a function of the dimensionless quantity  $\nu t^\alpha$  only<sup>2</sup>. Then, with  $x^\alpha = \nu t^\alpha$ , again from [Alòs et al.(2017)], we have that  $h(a, x)$  satisfies the fractional Riccati equation

$$D^\alpha h(a, x) = -\frac{1}{2} a(a+i) + i\rho a h(a, x) + \frac{1}{2} h(a, x)^2 \quad (2.3)$$

<sup>2</sup>This can also be seen directly from the rough Heston Riccati equation and the definition of the fractional derivative.

which can be re-expressed as

$$D^\alpha h(a, x) = \frac{1}{2} (h(a, x) - r_-) (h(a, x) - r_+) \quad (2.4)$$

with

$$A = \sqrt{a(a+i) - \rho^2 a^2}; \quad r_\pm = \{-i\rho a \pm A\}. \quad (2.5)$$

Without loss of generality, we will henceforth set  $\nu = 1$  and study the solution of the rescaled rough Heston Riccati equation (2.4). For small  $x$  we then have the expansion

$$h(a, x) = \sum_{j=0}^{\infty} \frac{\Gamma(1+j\alpha)}{\Gamma(1+(j+1)\alpha)} \beta_j(a) x^{(j+1)\alpha} \quad (2.6)$$

In integral form, (2.4) becomes

$$h(a, x) = \frac{1}{\Gamma(\alpha)} \int_0^x (x-y)^{\alpha-1} F[h(a, y)] dy \quad (2.7)$$

where

$$\begin{aligned} F[h] &= -\frac{1}{2} a(a+i) + i\rho a h + \frac{1}{2} h^2 \\ &= \frac{1}{2} (h - r_-) (h - r_+). \end{aligned} \quad (2.8)$$

### 3 Solving the rough Heston Riccati equation for long times

In general, the study of the large-time behavior of solutions of nonlinear fractional differential equations without known explicit solutions is difficult, and results are sparse in the literature. Using appropriate versions of the Grönwall and Bihari-LaSalle inequalities, solutions are known to decay to zero as power-type functions in some special cases [Kassim *et al.*(2016)].

When  $\alpha = 1$ , corresponding to the classical Heston case with no mean reversion, the Riccati equation (2.4) becomes

$$\partial_x h(a, x) = \frac{1}{2} (h(a, x) - r_+) (h(a, x) - r_-). \quad (3.1)$$

We recognize (3.1) as the classical Heston Riccati ODE, solved explicitly as on page 18 of [Gatheral(2006)] for example. The solution may be written as

$$h(a, x) = r_- \frac{1 - e^{-Ax}}{1 - \frac{r_-}{r_+} e^{-Ax}} \quad (3.2)$$

In analogy with this classical Heston solution, we expect that for  $a$  in  $\mathcal{A}$  (defined in Proposition 3.1 below),

$$\lim_{x \rightarrow \infty} h(a, x) = r_-. \quad (3.3)$$

In that case, for large  $x$ , we could linearize the fractional Riccati equation (2.4) as follows.

$$\begin{aligned} D^\alpha h(a, x) &= \frac{1}{2} (h(a, x) - r_-) (h(a, x) - r_+) \\ &\approx -\frac{1}{2} (r_+ - r_-) (h(a, x) - r_-) \\ &= -A (h(a, x) - r_-). \end{aligned} \quad (3.4)$$

The above linear fractional differential equation has the solution

$$h_{\infty}(a, x) = r_- [1 - E_{\alpha}(-A x^{\alpha})], \quad (3.5)$$

where  $E_{\alpha}(\cdot)$  is the Mittag-Leffler function (see A), as can be easily verified using (A.5). This heuristic argument is formalized in Proposition 3.1 below.

**Definition 3.1.** We henceforth define the strip in the complex plane relevant to the computation of option prices using (1.4) and to the computation of the leverage swap using (5.2):

$$\mathcal{A} = \left\{ z \in \mathbb{C} : \Re(z) \geq 0, -\frac{1}{1-\rho^2} \leq \Im(z) \leq 0 \right\} \quad (3.6)$$

where  $\Re$  and  $\Im$  denote real and imaginary parts respectively.

**Proposition 3.1.** Let  $h_{\infty}(a, x) = r_- [1 - E_{\alpha}(-A x^{\alpha})]$  where  $E_{\alpha}$  is the Mittag-Leffler function. Then, for  $x \in \mathbb{R}_{\geq 0}$  and  $a \in \mathcal{A}$ , as  $x \rightarrow \infty$ ,  $h_{\infty}(a, x)$  solves the rough Heston Riccati equation (2.4) up to an error term of  $\mathcal{O}(|A x^{\alpha}|^{-2})$ .

*Proof.* From (A.5), we have

$$D^{\alpha} [1 - E_{\alpha}(-A x^{\alpha})] = A E_{\alpha}(-A x^{\alpha}). \quad (3.7)$$

Then

$$\begin{aligned} D^{\alpha} h_{\infty}(a, x) &= r_- A E_{\alpha}(-A x^{\alpha}) \\ &= -A (h_{\infty}(a, x) - r_-) \\ &= -\frac{1}{2} (r_+ - r_-) (h_{\infty}(a, x) - r_-) \\ &= \frac{1}{2} (h_{\infty}(a, x) - r_+) (h_{\infty}(a, x) - r_-) - \frac{1}{2} (h_{\infty}(a, x) - r_-)^2. \end{aligned} \quad (3.8)$$

Also, from Corollary B.1, when  $a = u - \frac{i}{2}$ ,  $u \in \mathbb{R}_{>0}$  and  $x \in \mathbb{R}_{>0}$ , we have

$$E_{\alpha}(-A x^{\alpha}) = -\frac{1}{A} \frac{x^{-\alpha}}{\Gamma(1-\alpha)} + \mathcal{O}(|A x^{\alpha}|^{-2}), \quad x \rightarrow \infty. \quad (3.9)$$

Thus, as  $x \rightarrow \infty$ ,

$$h_{\infty}(a, x) - r_- = \frac{r_-}{A} \frac{x^{-\alpha}}{\Gamma(1-\alpha)} + \mathcal{O}(|A x^{\alpha}|^{-2}). \quad (3.10)$$

and from (3.8),

$$D^{\alpha} h_{\infty}(a, x) - \frac{1}{2} (h_{\infty}(a, x) - r_+) (h_{\infty}(a, x) - r_-) = \mathcal{O}(|A x^{\alpha}|^{-2}). \quad (3.11)$$

□

### 3.1 Large $x$ expansion

Recall that as  $x \rightarrow \infty$ , for  $a \in \mathcal{A}$ ,  $h_\infty(a, x) = r_- [1 - E_\alpha(-A x^\alpha)]$  solves the rough Heston Riccati equation (2.4) up to an error of order  $\mathcal{O}(|A x^\alpha|^{-2})$ . The form of the asymptotic expansion of  $E_\alpha(-A x^\alpha)$  in Lemma B.1 motivates the following ansatz for  $h(a, x)$  as  $x \rightarrow \infty$ :

$$h(a, x) = r_- \sum_{k=0}^{\infty} \gamma_k \frac{x^{-k\alpha}}{A^k \Gamma(1 - k\alpha)}. \quad (3.12)$$

Then

$$\frac{1}{r_-} D^\alpha h(a, x) = \sum_{k=0}^{\infty} \gamma_k \frac{x^{-(k+1)\alpha}}{A^k \Gamma(1 - (k+1)\alpha)} = A \sum_{k=1}^{\infty} \gamma_{k-1} \frac{x^{-k\alpha}}{A^k \Gamma(1 - k\alpha)}. \quad (3.13)$$

Also, from the fractional Riccati equation (2.4),

$$\begin{aligned} \frac{1}{r_-} D^\alpha h(a, x) &= \frac{1}{r_-} \frac{1}{2} (h(a, x) - r_-) (h(a, x) - r_+) \\ &= \frac{1}{r_-} \frac{1}{2} \left( r_- \sum_{k=1}^{\infty} \gamma_k \frac{x^{-k\alpha}}{A^k \Gamma(1 - k\alpha)} \right) \left( -2A + r_- \sum_{k=1}^{\infty} \gamma_k \frac{x^{-k\alpha}}{A^k \Gamma(1 - k\alpha)} \right) \\ &= \sum_{k=1}^{\infty} \gamma_k \frac{x^{-k\alpha}}{A^k \Gamma(1 - k\alpha)} \left( -A + \frac{1}{2} r_- \sum_{k=1}^{\infty} \gamma_k \frac{x^{-k\alpha}}{A^k \Gamma(1 - k\alpha)} \right). \end{aligned} \quad (3.14)$$

Equating (3.13) and (3.14) gives

$$\sum_{k=1}^{\infty} \gamma_{k-1} \frac{x^{-k\alpha}}{A^k \Gamma(1 - k\alpha)} = \sum_{k=1}^{\infty} \gamma_k \frac{x^{-k\alpha}}{A^k \Gamma(1 - k\alpha)} \left( -1 + \frac{r_-}{2A} \sum_{k=1}^{\infty} \gamma_k \frac{x^{-k\alpha}}{A^k \Gamma(1 - k\alpha)} \right). \quad (3.15)$$

This gives

$$\gamma_1 = -\gamma_0 = -1 \quad (3.16)$$

$$\gamma_2 = 1 + \frac{r_-}{2A} \frac{\Gamma(1 - 2\alpha)}{\Gamma(1 - \alpha)^2} \quad (3.17)$$

and so on. Indeed, the general recursion is given by

$$\gamma_k = -\gamma_{k-1} + \frac{r_-}{2A} \sum_{i,j=1}^{\infty} \mathbb{1}_{i+j=k} \gamma_i \gamma_j \frac{\Gamma(1 - k\alpha)}{\Gamma(1 - i\alpha) \Gamma(1 - j\alpha)}. \quad (3.18)$$

## 4 Rational approximations

Given integers  $m, n \geq 0$ , and a formal power series  $f(z) = \sum_{j=0}^{\infty} a_j z^j$  with complex coefficients and a certain radius of convergence, for some (often unknown) function  $f$ , the  $(m, n)$  Padé approximant to  $f$  is a rational function  $f^{(m,n)}(z) = P(z)/Q(z)$ , where  $P(z) = \sum_{i=0}^m p_m z^m$  and  $Q(z) = \sum_{j=0}^n q_n z^n$  are polynomials of degree at most  $m$  and  $n$ , respectively, such that  $Q(z)$  is not identically zero, and  $f(z)Q(z) - P(z) = \mathcal{O}(z^{m+n+1})$ . The last equation can be easily restated as a system of  $m + n + 1$  linear equations in  $(m + 1) + (n + 1)$  coefficients

of the polynomials  $P(z)$  and  $Q(z)$ , eventually leading to the unique  $f^{(m,n)}$ . Dating back to the works of Hermite and Padé in the 1890s, Padé approximants have been extensively used across mathematics (*e.g.* practical approximations of special functions, continued fractions and transcendence in number theory, numerical solutions of PDEs) and in physics (*e.g.* scattering theory, critical phenomena in statistical physics, singularity detection in dynamical systems) [Baker *et al.*(1996), Yamada & Ikeda(2014)]. In these applications, Padé approximants typically turn out to be excellent approximations to  $f$ , even beyond the domain of convergence of the power series of  $f$ , used to construct the approximants.

There exists an extensive literature [Lubinsky(2003)] on the convergence of Padé approximants, the theory of which is quite intricate. For example, according to de Montessus de Ballore's theorem [Baker *et al.*(1996)], if  $f$  is analytic in a ball centered at zero, except for poles of total multiplicity  $n$ , the sequence  $\{f^{(m,n)}\}_{m=1}^{\infty}$ , for fixed  $n$ , converges uniformly to  $f$  in compact subsets omitting the poles. However, in general, without prior knowledge of the number of poles  $n$ , or other specific properties of  $f$ , de Montessus de Ballore's theorem cannot be applied.

According to the Baker-Gammel-Wills conjecture, under certain conditions, the *diagonal* Padé approximants  $\{f^{(n,n)}\}_{n=1}^{\infty}$  converge uniformly to  $f$ . Quoting from the excellent review article of [Lubinsky(2014)]:

Physicists such as George Baker in the 1960's endeavoured to surmount the problem of spurious poles. They noted that these typically affect convergence only in a small neighborhood, and there were usually very few of these "bad" approximants. Thus, one might compute  $[n/n], n = 1, 2, 3, \dots, 50$ , and find a definite convergence trend in 45 of the approximants, with 5 of the 50 approximants displaying pathological behavior. Moreover, the 5 bad approximants could be distributed anywhere in the 50, and need not be the first few. Nevertheless, after omitting the "bad" approximants, one obtained a clear convergence trend. This seemed to be a characteristic of the Padé method, and led to a famous conjecture (the Baker-Gammel-Wills conjecture).

Sadly, a clever counterexample was given in [Lubinsky(2003)]. According to Nuttall-Pommerenke's theorem [Lubinsky(2003)] however, there does exist a subsequence of  $\{f^{(n,n)}\}_{n=1}^{\infty}$  that converges almost everywhere.

Uniform convergence of Padé approximants for the Mittag-Leffler function  $E_{\alpha}(z)$  was proved in [Starovoitov & Starovoitova(2007)] on the compact set  $\{|z| \leq 1\}$ . While Padé approximants are better than their corresponding truncated Taylor series, they are not necessarily compatible with the asymptotic behavior of the Mittag-Leffler function for larger arguments (see Lemma B.1). Global rational approximations for transcendental functions were derived in [Winitzki(2003)] using multipoint Padé approximants. The idea is quite natural as one tries to find the  $(m, n)$  Padé approximant that matches the series expansions of a function in question both at zero and at infinity, in the hope that the rational approximation will be accurate everywhere in between. This method has subsequently been successfully applied in [Atkinson & Osseiran(2011)] to the Mittag-Leffler function and then in [Zeng & Chen(2015)] to the generalized Mittag-Leffler function. Although our integral equation (2.7) is not linear, it is also worth mentioning that diagonal Padé approximants to the solution of linear integral equations converge to the exact solution under some mild conditions on the kernel, see for example Chapter 9 of [Baker *et al.*(1996)].

#### 4.1 Application to the rough Heston Riccati equation

In previous sections, we derived the short-time and long-time asymptotics of  $h$ . Following the same approach as [Atkinson & Osseiran(2011)], we can now therefore compute global rational approximations to  $h(a, x)$  of the form

$$h^{(m,n)}(a, x) = \frac{\sum_{i=1}^m p_i y^i}{\sum_{j=0}^n q_j y^j} \quad (4.1)$$

with  $y = x^\alpha$ , that match both (2.6) and (3.12).

Only the diagonal approximants  $h^{(n,n)}$  are admissible approximations of  $h$ . To see this, note that as  $x \rightarrow \infty$ , from (3.12) and (3.16),

$$h^{(m,n)}(a, x) \sim \frac{p_m}{q_n} y^{m-n} \rightarrow r_- \quad (4.2)$$

with  $0 < |r_-| < \infty$  only if  $m = n$ . Given the approximation  $h^{(n,n)}$  of  $h$ , we then approximate  $D^\alpha h$  by  $F[h] = \frac{1}{2} (h - r_+) (h - r_-)$ .

From various numerical experiments, some of which are detailed in Section 5, the particular approximation  $h^{(3,3)}$  seems to be very close to the true solution for reasonable choices of model parameters. Though the excellent quality of the global approximation  $h^{(3,3)}$  might at first seem very surprising, it is perhaps less surprising in the context of the story of diagonal Padé approximants told above. Accordingly, we work out the  $m = n = 3$  case in detail, whilst noting that the procedure we present may be easily generalized to lower and higher order approximations.

From (2.6), we have the series expansion of  $h$  for small  $y$ :

$$h_s(y) = b_1 y + b_2 y^2 + b_3 y^3 + \mathcal{O}(y^4). \quad (4.3)$$

From (3.12), we have the series expansion of  $h$  for large  $y$ :

$$h_\ell(y) = g_0 + \frac{g_1}{y} + \frac{g_2}{y^2} + \mathcal{O}\left(\frac{1}{y^3}\right). \quad (4.4)$$

Matching the coefficients of the rational approximation<sup>3</sup>

$$h^{(3,3)}(y) = \frac{p_1 y + p_2 y^2 + p_3 y^3}{1 + q_1 y + q_2 y^2 + q_3 y^3} \quad (4.5)$$

to  $h_s(y)$  and  $h_\ell(y)$  respectively, forces the coefficients  $b_i, g_j$  to satisfy:

$$p_1 = b_1 \quad (4.6)$$

$$p_2 - p_1 q_1 = b_2 \quad (4.7)$$

$$p_1 q_1^2 - p_1 q_2 - p_2 q_1 + p_3 = b_3 \quad (4.8)$$

$$\frac{p_3}{q_3} = g_0 \quad (4.9)$$

$$\frac{p_2 q_3 - p_3 q_2}{q_3^2} = g_1 \quad (4.10)$$

$$\frac{p_1 q_3^2 - p_2 q_2 q_3 - p_3 q_1 q_3 + p_3 q_2^2}{q_3^3} = g_2. \quad (4.11)$$

<sup>3</sup>Wlog, the constant term  $q_0$  in the denominator is set to 1.



The solution of this system of six equations with six unknowns is

$$p_1 = b_1 \quad (4.12)$$

$$p_2 = \frac{b_1^3 g_1 + b_1^2 g_0^2 + b_1 b_2 g_0 g_1 - b_1 b_3 g_0 g_2 + b_1 b_3 g_1^2 + b_2^2 g_0 g_2 - b_2^2 g_1^2 + b_2 g_0^3}{b_1^2 g_2 + 2b_1 g_0 g_1 + b_2 g_0 g_2 - b_2 g_1^2 + g_0^3} \quad (4.13)$$

$$p_3 = \frac{g_0 (b_1^3 + 2b_1 b_2 g_0 + b_1 b_3 g_1 - b_2^2 g_1 + b_3 g_0^2)}{b_1^2 g_2 + 2b_1 g_0 g_1 + b_2 g_0 g_2 - b_2 g_1^2 + g_0^3} = g_0 q_3 \quad (4.14)$$

$$q_1 = \frac{b_1^2 g_1 - b_1 b_2 g_2 + b_1 g_0^2 - b_2 g_0 g_1 - b_3 g_0 g_2 + b_3 g_1^2}{b_1^2 g_2 + 2b_1 g_0 g_1 + b_2 g_0 g_2 - b_2 g_1^2 + g_0^3} \quad (4.15)$$

$$q_2 = \frac{b_1^2 g_0 - b_1 b_2 g_1 - b_1 b_3 g_2 + b_2^2 g_2 + b_2 g_0^2 - b_3 g_0 g_1}{b_1^2 g_2 + 2b_1 g_0 g_1 + b_2 g_0 g_2 - b_2 g_1^2 + g_0^3} \quad (4.16)$$

$$q_3 = \frac{b_1^3 + 2b_1 b_2 g_0 + b_1 b_3 g_1 - b_2^2 g_1 + b_3 g_0^2}{b_1^2 g_2 + 2b_1 g_0 g_1 + b_2 g_0 g_2 - b_2 g_1^2 + g_0^3}. \quad (4.17)$$

**Remark 4.1.** Since  $\beta_0(a) = -\frac{1}{2} a(a+i)$  is an overall prefactor of any rational approximation matching (2.6) for small  $x$ , we obviously have  $h^{(n,n)}(0, x) = h^{(n,n)}(-i, x) = 0$  for any diagonal rational approximation  $h^{(n,n)}$ . It follows from (2.4) that  $D^\alpha h^{(n,n)}(0, x) = D^\alpha h^{(n,n)}(-i, x) = 0$ , as required to satisfy the total probability and martingale conditions on the cumulant generating function (CGF).

## 5 Numerical results

In the following, unless specifically otherwise stated, we assume the following realistic rough Heston parameters:

$$H = 0.05; \nu = 0.4; \rho = -0.65. \quad (5.1)$$

### 5.1 Convergence of the Adams scheme

In the literature, it is often assumed that the Adams scheme converges with relatively few time steps, 200 say. From our numerical experiments, this is true when  $H$  is large enough, for example when  $H = \frac{1}{2}$ . However, when  $H$  is small, as we find when analyzing volatility time series data or estimating it from the implied volatility surface, convergence is much slower. In Figure 5.1, we plot  $h(a, x)$  estimated using the Adams scheme with various choices of the number of time steps. We see that when  $H = 0.05$ , we need thousands of time steps to achieve convergence of the Adams scheme to the solution of the rough Heston Riccati equation.

### 5.2 Comparison of rational approximations

We now approximate  $h(a, x)$  using the Adams scheme with 50,000 time steps and study the accuracy of rational approximations  $h^{(n,n)}(a, x)$  to  $h(a, x)$  for  $n = 2, 3, 4$ . Note in particular that all of these rational approximations are at least as fast to compute as the classical Heston solution. Results for the particular choice  $a = 3 - i/2$  with rough Heston parameters (5.1) are plotted in Figure 5.2. By inspection,  $h^{(3,3)}$  is by far the best of these approximate solutions.

As for higher order approximants, though Nuttall-Pommerenke's theorem guarantees the existence of a subsequence of  $\{h^{(n,n)}\}_{n=1}^\infty$  that converges almost everywhere, there is no known

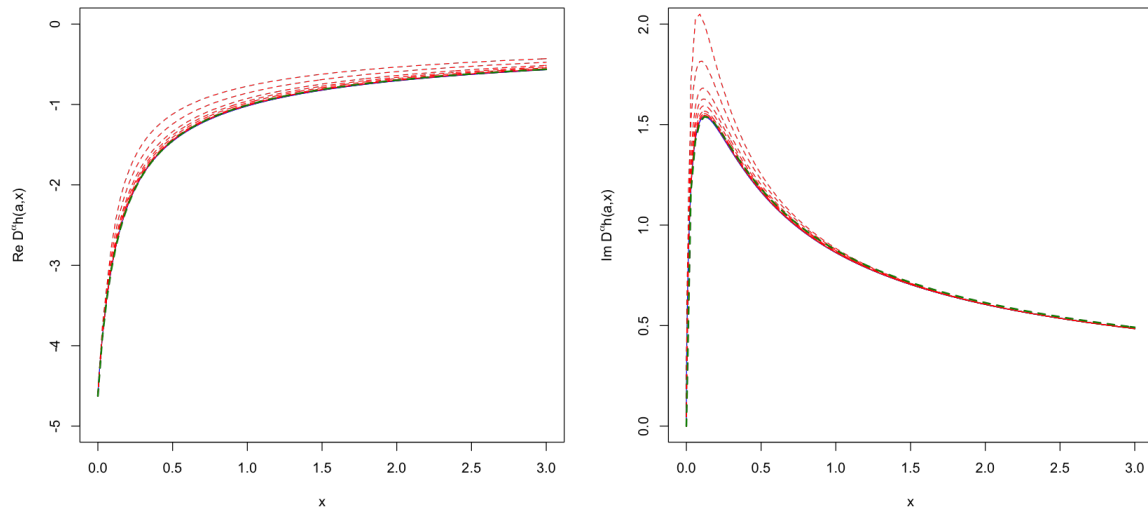


Figure 5.1: In the left panel  $\Re D^\alpha h(3 - i/2, x)$  and in the right panel  $\Im D^\alpha h(3 - i/2, x)$ ; solid blue lines are the Adams scheme estimate with 50,000 steps; dashed green lines are the rational approximation  $h^{(3,3)}$ . Dashed red lines are Adams scheme estimates with respectively 100, 200, 500, 1,000, 2,000, 5,000, 10,000 and 20,000 steps. Adams scheme estimates using 20,000 and 50,000 steps are visually indistinguishable from the rational approximation  $h^{(3,3)}$ .

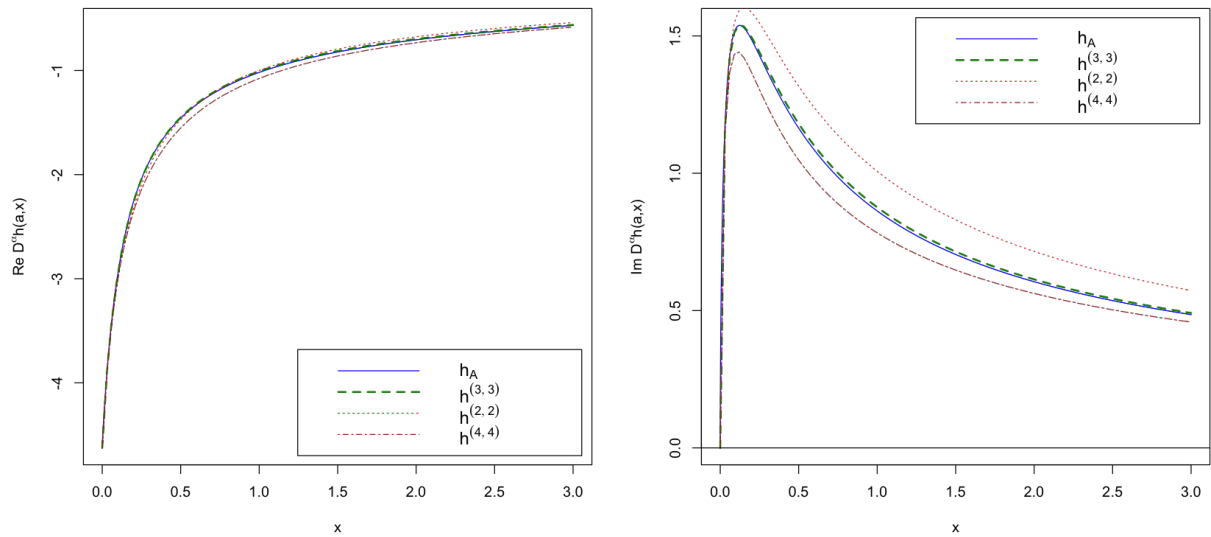


Figure 5.2: In the left panel  $\Re D^\alpha h(3 - i/2, x)$  and in the right panel  $\Im D^\alpha h(3 - i/2, x)$ .  $h^{(3,3)}$  is almost indistinguishable from the 50,000 step Adams estimate and significantly better than the alternative rational approximations.

practical recipe to find the members of this subsequence. Naturally the coefficients of the

higher order diagonal approximants become successively harder to compute in closed form. And since the formulae are more complex, the functions when implemented take longer to compute. Thus, even if, for example,  $h^{(7,7)}$  were to be a better approximation than  $h^{(3,3)}$ , it would be much slower to compute and  $h^{(3,3)}$  would likely be the approximation of choice in practice.

### 5.3 Parameter dependence of approximation quality

So far, we have assessed the quality of our best rational approximation  $h^{(3,3)}$  with the realistic but fixed set of parameters (5.1). It is natural to wonder whether or not  $h^{(3,3)}$  is such a good approximation to  $h$  for all possible parameter choices. We now fix  $a = 3 - i/2$  and plot  $h(a, x)$  for various values of  $H$ . In Figure 5.3, we see that keeping other rough Heston parameters fixed,  $h^{(3,3)}$  approximates  $h$  almost perfectly when  $H = 0$  but that the approximation quality deteriorates as  $H$  increases. Though this deterioration in approximation quality might seem to imply that it would be inappropriate to use the rational approximation  $h^{(3,3)}$  in the  $H \approx 1/2$  regime (the classical Heston model with no mean reversion), with reasonable parameters, it turns out that the approximate volatility smile is nevertheless surprisingly close to the true classical Heston smile.

### 5.4 The leverage swap

As discussed in Section 5.1, the Adams scheme converges slowly. To assess the error in rational approximations to  $h(a, x)$ , it would be ideal if we could compare some quantity computed using a rational approximation with the same quantity computable in the rough Heston model in closed form. The leverage swap, the difference between a gamma swap and a variance swap is such a quantity.

From Corollary 5.1 of [Alòs et al.(2017)], the fair value of the ~~leverage swap~~ in the rough Heston model is given by

$$\mathcal{L}_t(T) = -2i\rho\nu \int_t^T h'(-i, T-u) \xi_t(u) du \quad (5.2)$$

where  $h'(a, t) = \partial_a h(a, t)$ . Moreover, from Corollary 5.2 of [Alòs et al.(2017)], under rough Heston, the leverage swap has the closed-form expression

$$\mathcal{L}_t(T) = \int_t^T \xi_t(u) \{E_\alpha(\rho\nu\tau^\alpha) - 1\} du \quad (5.3)$$

where as before,  $E_\alpha(\cdot)$  is the Mittag-Leffler function. This suggests another test of the quality of the rational approximation  $h^{(3,3)}$ . Specifically, we may compute the approximation

$$\mathcal{L}_t^{(3,3)}(T) = -2i\rho\nu \int_t^T h^{(3,3)}(-i, T-u) \xi_t(u) du \quad (5.4)$$

and compare with the exact computation of  $\mathcal{L}_t(T)$ . As in [Alòs et al.(2017)], we assume a flat forward variance curve and normalize the leverage swap by the variance swap to obtain the normalized leverage swap  $L_t(T) = \mathcal{L}_t(T)/w_t(T) = E_{\alpha,2}(\rho\nu\tau^\alpha) - 1$ , where  $w_t(T) = \int_t^T \xi_t(u) du$  and  $E_{\alpha,2}(\cdot)$  is a generalized Mittag-Leffler function (see A). The approximate normalized leverage swaps  $L_t^{(n,n)}(T)$  are defined similarly. Approximate and exact normalized leverage

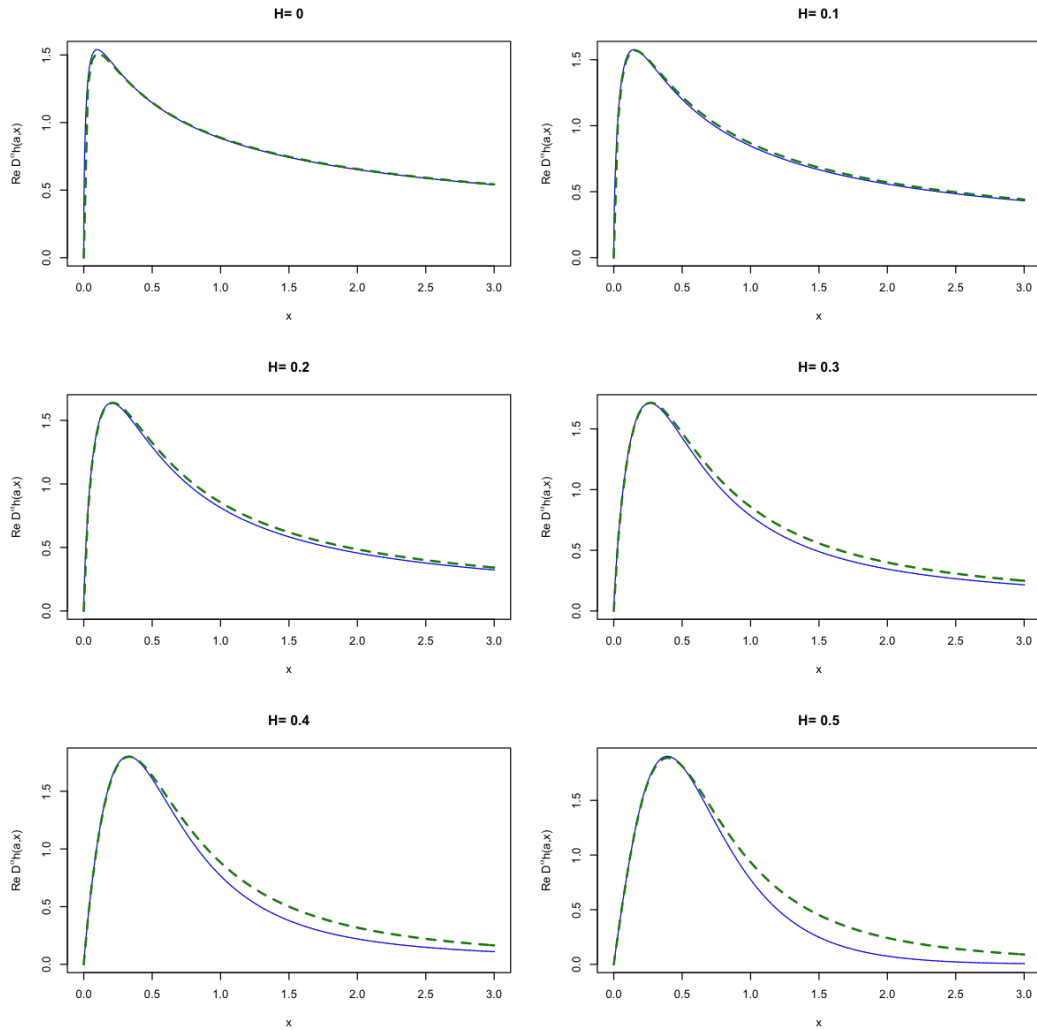


Figure 5.3:  $\Re D^\alpha h(3 - i/2, x)$  computed for various values of  $H$ ; solid blue lines are Adams scheme estimates with 10,000 steps; dashed green lines are the rational approximations  $h^{(3,3)}$ . The rational approximation and the numerical solution are almost indistinguishable when  $H = 0$ .

swaps are plotted in Figure 5.4. Agreement between  $L_t^{(3,3)}(T)$  and  $L_t(T)$  is so good that it is only really possible to detect the error by plotting the ratio of the true and approximate solutions. We therefore plot the ratio  $L_t^{(3,3)}(T)/L_t(T)$  in the right panel of Figure 5.4 together with the ratios  $L_t^{(2,2)}(T)/L_t(T)$  and  $L_t^{(4,4)}(T)/L_t(T)$  (with obvious notation); consistent with the above results for  $h^{(3,3)}$ ,  $L_t^{(3,3)}(T)$  does much better than the other two. The maximum relative error in  $L_t^{(3,3)}(T)$  over this range of expirations is only 0.3%.

Now fix  $\nu = 0.4$  and  $\tau = 1$ . For  $n = 2, 3, 4$ , define the leverage swap relative approximation error as

$$\epsilon(n) = \log \left( \frac{\mathcal{L}^{(n,n)}}{\mathcal{L}} \right). \quad (5.5)$$

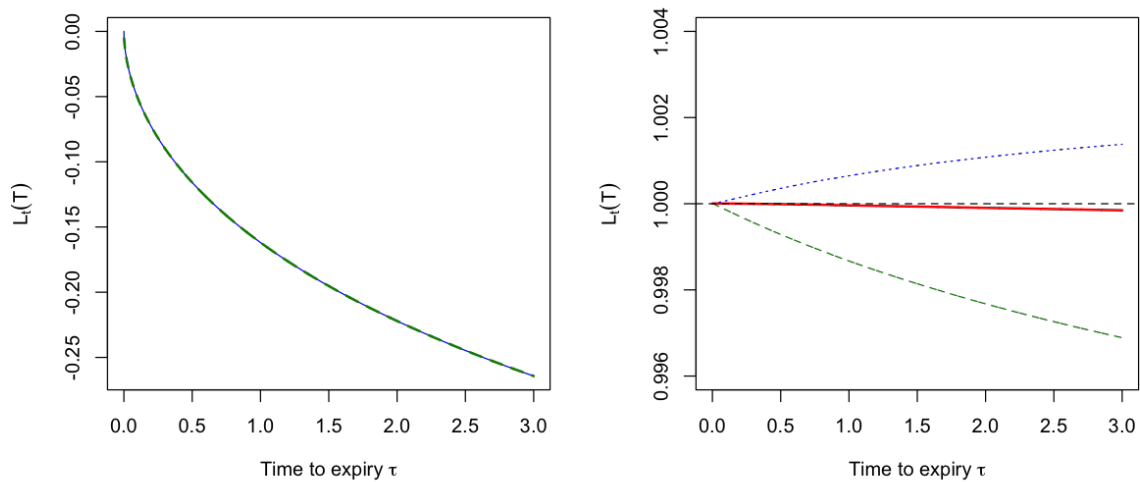


Figure 5.4: In the left panel, we compare the approximate normalized leverage swap  $L^{(3,3)} = \mathcal{L}^{(3,3)}/w$  where  $\mathcal{L}^{(3,3)}$  is from (5.4) with the exact solution  $L = \mathcal{L}/w = E_{\alpha,2}(\rho \nu \tau^\alpha) - 1$ . The solid blue line is  $L$ ; the green dashed line is  $L^{(3,3)}$ ;  $L$  and  $L^{(3,3)}$  are almost indistinguishable. In the right panel, we plot the ratio of various approximations of the normalized leverage swap to the exact solution  $L$ . The solid red line is  $L^{(3,3)}/L$ ; the dashed green line is  $L^{(2,2)}/L$ ; the dotted blue line is  $L^{(4,4)}/L$ .

How do the errors  $\epsilon(n)$  depend on  $\rho$  and  $H$ ? In Figure 5.5, we see that  $\mathcal{L}^{(3,3)}$  is a very good approximation to  $\mathcal{L}$  for all  $\rho \in [-1, 1]$ , and really excellent when  $\rho \leq 0$ , which is the region of practical interest for option pricing. Moreover, from these plots, we observe that  $h^{(3,3)}$  is consistently better than the other two rational approximations whenever errors are significant. When  $\rho$  is close to zero, all three rational approximations are excellent.

## 5.5 Implied volatility smiles

Recall that our ultimate objective is to find a good rational approximation to the solution  $h(a, x)$  of the fractional Riccati equation suitable for pricing options. We adopt the same rough Heston parameters as in [El Euch *et al.* (2017)] obtained from calibration of the model to SPX options as of May 19, 2017, computing implied volatilities for all options with nonzero bids. In Figure 5.6, we see that approximate smiles computed using  $h^{(3,3)}$  and smiles generated using the Adams scheme with 200 steps are almost indistinguishable. Once again, we stress that these approximate smiles are at least as fast to compute as the equivalent classical Heston smiles. Moreover, our numerical experiments indicate that with this choice of parameters, the Adams scheme with 200 steps generates greater errors than the rational approximation  $h^{(3,3)}$ .

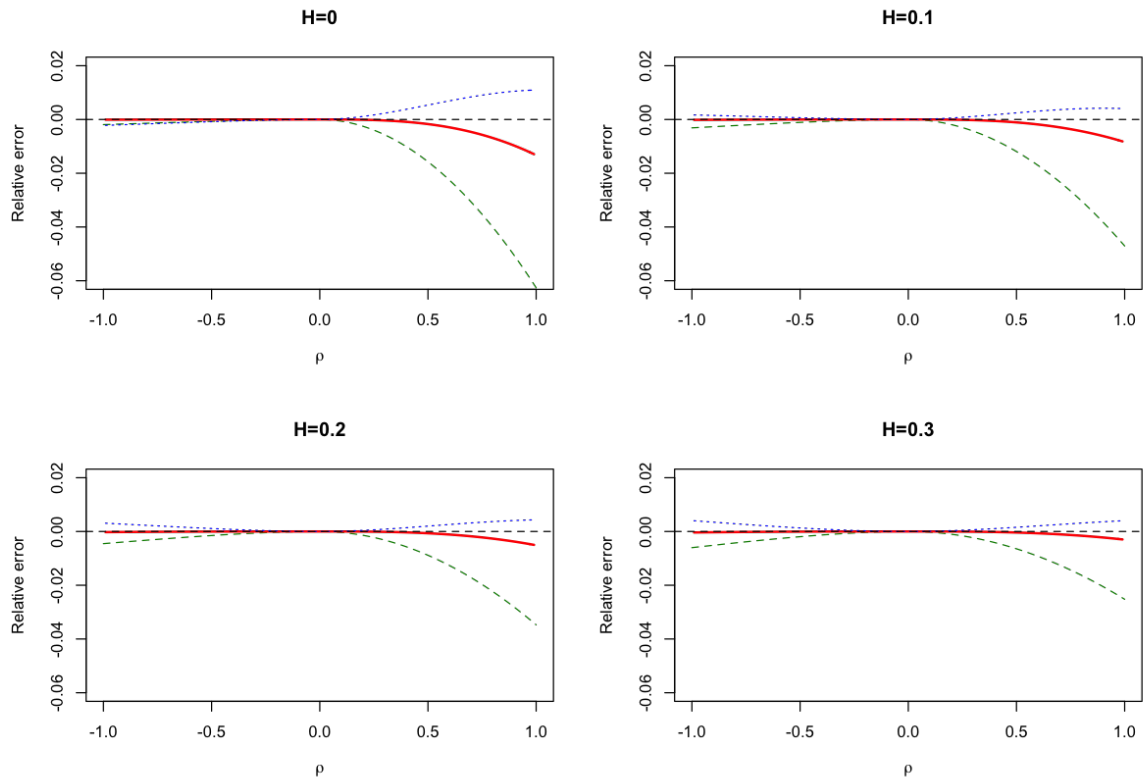


Figure 5.5: For various values of  $H$ , we plot the relative approximation errors  $\epsilon(n)$  defined in (5.5) against the correlation  $\rho$ . The solid red line is  $\epsilon(3)$ ; the dashed green line is  $\epsilon(2)$ ; the dotted blue line is  $\epsilon(4)$ .

## 6 Summary and conclusions

Starting from short-time and long-time expansions of the solution  $h$  of the rough Heston Riccati equation (1.3), we have constructed various global rational approximations to  $h$ , valid in a region of the complex plane relevant to the valuation of European options. One such rational approximation,  $h^{(3,3)}$ , turned out to be particularly simple and accurate, especially for the empirically relevant  $H$  close to zero case, as demonstrated by numerical experiments. We further showed that this rational approximation  $h^{(3,3)}$  gave results that were more accurate than the standard numerical method, the Adams scheme, with any reasonable number of time steps. Moreover  $h^{(3,3)}$  is at least as fast to compute as the classical Heston solution.

Why  $h^{(3,3)}$  is such an outstandingly good approximation to the solution of the rough Heston Riccati equation is left for further research. As we mentioned in Section 4, this is perhaps yet another instance of a phenomenon already noted in the Padé approximant literature that is not yet well understood.

Finally, the rough Heston Riccati equation is just one example of a nonlinear fractional differential equation. Perhaps our technique of matching short- and long-time expansions of the solution using rational approximations may be applicable to a wider class of stochastic volatility models and more generally, to a wider class of fractional differential equations, particularly topical in physics.

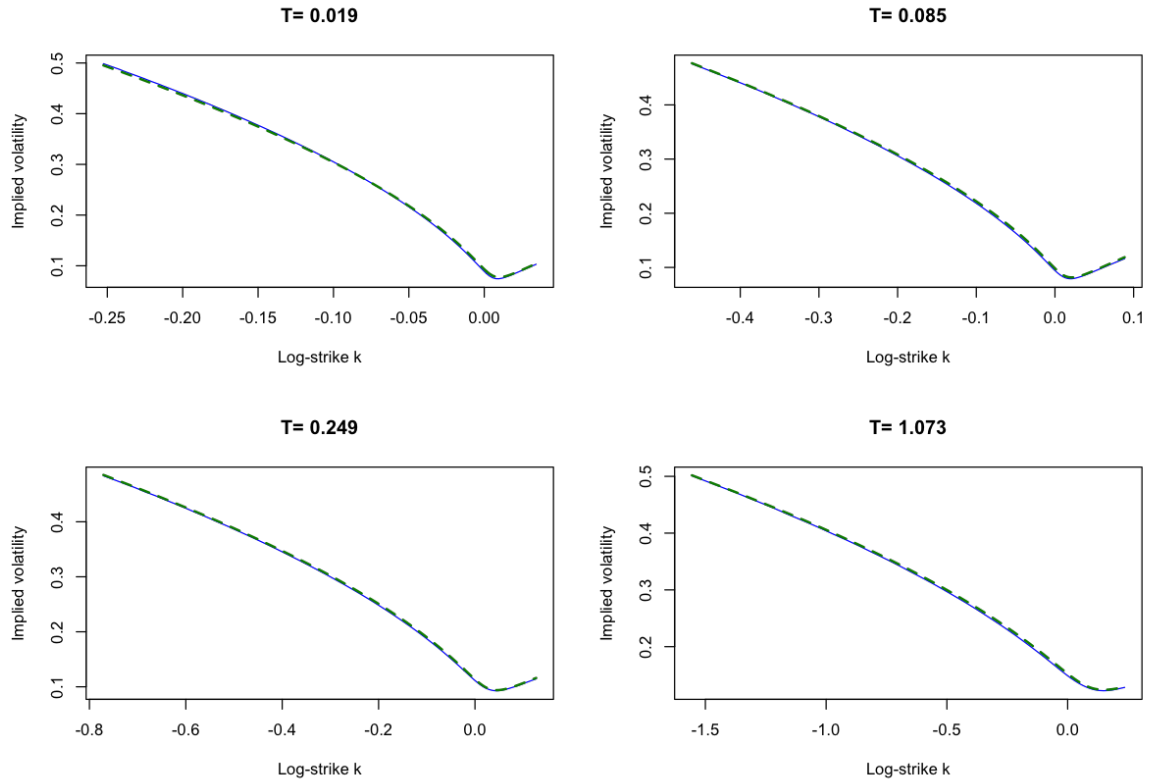


Figure 5.6: Representative SPX volatility smiles as of May 19, 2017, with time to expiration in years. Blue smiles are from the rough Heston model calibrated using the Adams scheme; green dashed smiles are from the  $h^{(3,3)}$  rational approximation to  $h$ . The approximate and exact smiles are indistinguishable on this plot.

## A Some fractional calculus

We define the fractional integral of order  $r \in (0, 1]$  of a function  $f$  as

$$I^r f(t) = \frac{1}{\Gamma(r)} \int_0^t (t-s)^{r-1} f(s) ds, \quad (\text{A.1})$$

whenever the integral exists, and the fractional derivative of order  $r \in [0, 1)$  as

$$D^r f(t) = \frac{1}{\Gamma(1-r)} \frac{d}{dt} \int_0^t (t-s)^{-r} f(s) ds, \quad (\text{A.2})$$

whenever it exists.

With these definitions, it is straightforward to verify that

$$D^\alpha t^{k\alpha} = \frac{\Gamma(1+k\alpha)}{\Gamma(1+(k-1)\alpha)} t^{(k-1)\alpha}. \quad (\text{A.3})$$

The Mittag-Leffler function, as defined in for example equation (1.55) of [Podlubny(1998)], is given by

$$E_\alpha(C t^\alpha) = \sum_{k=0}^{\infty} \frac{C^k t^{k\alpha}}{\Gamma(k\alpha + 1)}. \quad (\text{A.4})$$

Using (A.3) we obtain

$$\begin{aligned} D^\alpha [E_\alpha(C t^\alpha) - 1] &= D^\alpha \sum_{k=1}^{\infty} \frac{C^k t^{k\alpha}}{\Gamma(1+k\alpha)} \\ &= \sum_{k=1}^{\infty} \frac{C^k t^{(k-1)\alpha}}{\Gamma(1+(k-1)\alpha)} \\ &= C E_\alpha(C t^\alpha). \end{aligned} \quad (\text{A.5})$$

Also, the generalized Mittag-Leffler function, as defined in for example equation (1.56) of [Podlubny(1998)], is given by

$$E_{\alpha,\beta}(C t^\alpha) = \sum_{k=0}^{\infty} \frac{C^k t^{k\alpha}}{\Gamma(k\alpha + \beta)}. \quad (\text{A.6})$$

## B Asymptotic expansion of the Mittag-Leffler function

The following lemma is a straightforward corollary of Theorem 1.4 of [Podlubny(1998)].

**Lemma B.1.** *Let  $0 < \alpha \leq 1$  and  $\mu \in \mathbb{R}$  be such that*

$$\frac{\pi\alpha}{2} < \mu < \pi\alpha. \quad (\text{B.1})$$

*Then, for any integer  $p > 0$ , the following expansion holds:*

$$E_\alpha(z) = - \sum_{k=1}^p \frac{z^{-k}}{\Gamma(1-k\alpha)} + \mathcal{O}(|z|^{-1-p}), \quad |z| \rightarrow \infty, \quad \mu \leq |\arg(z)| \leq \pi. \quad (\text{B.2})$$

**Lemma B.2.** *Let  $0 < \alpha \leq 1$ . Further let  $a = u + iy$  with  $u \in \mathbb{R}_{\geq 0}$ ,  $y \in [-\frac{1}{1-\rho^2}, 0]$  and let  $A = \sqrt{a(a+i) - \rho^2 a^2}$ . Then for any  $x \in \mathbb{R}_{>0}$ ,*

$$|\arg(-A x^\alpha)| \in \left[ \frac{3\pi}{4}, \pi \right]. \quad (\text{B.3})$$

*Proof.* Let  $\bar{\rho} = \sqrt{1 - \rho^2}$ . Then

$$\Re(A^2) = \bar{\rho}^2 (u^2 - y^2) - y = \bar{\rho}^2 u^2 - y(\bar{\rho}^2 y + 1) \quad (\text{B.4})$$

$$\Im(A^2) = u(2\bar{\rho}^2 y + 1). \quad (\text{B.5})$$

Since  $\Re(A^2)$  is positive,  $\arg A^2 \in [-\frac{\pi}{2}, \frac{\pi}{2}]$  and so  $\arg A \in [-\frac{\pi}{4}, \frac{\pi}{4}]$ . Both  $x$  and  $\alpha$  are positive real numbers. It follows that

$$|\arg(-A x^\alpha)| \in \left[ \frac{3\pi}{4}, \pi \right]. \quad (\text{B.6})$$

□

**Corollary B.1.** *Let  $0 < \alpha \leq 1$ . Further let  $a = u + iy$  with  $u \in \mathbb{R}_{>0}$  and  $y \in [-1/(1-\rho^2), 0]$ . Further let  $A = \sqrt{a(a+i) - \rho^2 a^2}$ . For any positive integer  $p$  and  $x \in \mathbb{R}_{>0}$ ,*

$$E_\alpha(-A x^\alpha) = \sum_{k=1}^p \frac{(-1)^{k-1}}{A^k} \frac{x^{-k\alpha}}{\Gamma(1-k\alpha)} + \mathcal{O}(|A x^\alpha|^{-1-p}), \quad x \rightarrow \infty. \quad (\text{B.7})$$

*Proof.* Apply Lemma B.1 and Lemma B.2 with  $\mu = \frac{3}{4}\pi\alpha$ . □



## References

- [Abi Jaber *et al.*(2017)] E. Abi Jaber, M. Larsson & S. Pulido (2017) Affine Volterra processes, *arXiv:1708.08796*.
- [Abi Jaber & El Euch(2018)] E. Abi Jaber & O. El Euch (2018) Multi-factor approximation of rough volatility models, *arXiv:1801.10359*.
- [Alòs *et al.*(2017)] E. Alòs, J. Gatheral & R. Radoičić (2017) Exponentiation of conditional expectations under stochastic volatility, *SSRN 2983180*.
- [Atkinson & Osseiran(2011)] C. Atkinson & A. Osseiran (2011) Rational solutions for the time-fractional diffusion equation, *SIAM Journal on Applied Mathematics* **71** (1), 92–106.
- [Baker *et al.*(1996)] G. A. Baker, G. A. Baker Jr., P. Graves-Morris & S. S. Baker (1996) *Padé approximants*. Cambridge: Cambridge University Press.
- [Bhrawy *et al.*(2015)] A. H. Bhrawy, T. M. Taha & J. A. Tenreiro Machado (2015) A review of operational matrices and spectral techniques for fractional calculus, *Nonlinear Dynamics* **81** (3), 1023–1052.
- [Callegaro *et al.*(2018)] G. Callegaro, M. Grasselli & G. Pagès (2018) Rough but not so tough: fast hybrid schemes for fractional Riccati equations, *arXiv:1805.12587*.
- [Cang *et al.*(2009)] J. Cang, Y. Tan, H. Xu & S. Liao (2009) Series solutions of non-linear Riccati differential equations with fractional order, *Chaos, Solitons and Fractals* **40** (1), 1–9.
- [Diethelm *et al.*(2004)] K. Diethelm, N. J. Ford & A. D. Freed (2004) Detailed error analysis for a fractional Adams method, *Numerical Algorithms* **36** (1), 31–52.
- [El Euch & Rosenbaum(2019)] O. El Euch & M. Rosenbaum (2019) The characteristic function of rough Heston models. *Mathematical Finance*, **29** (1), 3–38.
- [El Euch *et al.*(2017)] O. El Euch, J. Gatheral & M. Rosenbaum (2017) Roughening Heston, *SSRN 3116887*.
- [Gatheral(2006)] J. Gatheral (2006) *The Implied Volatility Surface: A Practitioner's Guide*. New York: Wiley.
- [Gatheral & Keller-Ressel(2018)] J. Gatheral & M. Keller-Ressel (2018) Affine forward variance models, *arXiv:1801.06416*.
- [Jaisson & Rosenbaum(2016)] T. Jaisson & M. Rosenbaum (2016) Rough fractional diffusions as scaling limits of nearly unstable heavy tailed Hawkes processes, *The Annals of Applied Probability* **26** (5), 2860–2882.
- [Kassim *et al.*(2016)] M. D. Kassim, K. M. Furati & N.-E. Tatar (2016) Asymptotic behavior of solutions to nonlinear initial-value fractional differential problems, *Electronic Journal of Differential Equations*, **291**, 1–14.
- [Lewis(2000)] A. L. Lewis (2000) *Option Valuation under Stochastic Volatility with Mathematica code*. Newport Beach: Finance Press.

- [Lubinsky(2003)] D. S. Lubinsky (2003) Rogers-Ramanujan and the Baker-Gammel-Wills (Padé) conjecture, *Annals of Mathematics* **157** (3), 847–889.
- [Lubinsky(2014)] D. S. Lubinsky (2014) Reflections on the Baker–Gammel–Wills (Padé) Conjecture. In: *Analytic Number Theory, Approximation Theory, and Special Functions* (G. V. Milovanović & M. Th. Rassias, eds.), 561–571. New York: Springer.
- [Momani & Shawagfeh(2006)] S. Momani & N. Shawagfeh (2006) Decomposition method for solving fractional Riccati differential equations, *Applied Mathematics and Computation* **182** (2), 1083–1092.
- [Odibat & Momani(2006)] Z. M. Odibat & S. Momani (2006) Application of variational iteration method to nonlinear differential equations of fractional order, *International Journal of Nonlinear Sciences and Numerical Simulation* **7** (1), 27–34.
- [Odibat & Momani(2008)] Z. M. Odibat & S. Momani (2008) Modified homotopy perturbation method: application to quadratic Riccati differential equation of fractional order, *Chaos, Solitons and Fractals* **36** (1), 167–174.
- [Podlubny(1998)] I. Podlubny (1998) *Fractional Differential Equations: An Introduction to Fractional Derivatives, Fractional Differential Equations, to Methods of their Solution and some of their Applications*, San Diego: Academic Press.
- [Starovoitov & Starovoitova(2007)] A. P. Starovoitov & N. A. Starovoitova (2007) Padé approximants of the Mittag-Leffler functions, *Sbornik: Mathematics* **198** (7), 1011–1023.
- [Winitzki(2003)] S. Winitzki (2003) Uniform approximations for transcendental functions. In: *International Conference on Computational Science and its Applications*, (V. Kumar, M. L. Gavrilova, C. J. Tan & P. L’Ecuyer, eds.), 780–789. Heidelberg: Springer.
- [Yamada & Ikeda(2014)] H. S. Yamada & K. S. Ikeda (2014) A numerical test of Padé approximation for some functions with singularity, *International Journal of Computational Mathematics* **587430**.
- [Zeng & Chen(2015)] C. Zeng & Y. Q. Chen (2015) Global Padé approximations of the generalized Mittag-Leffler function and its inverse, *Fractional Calculus and Applied Analysis*, **18** (6) 1492–1506.